Subject classification: 61.43

NEW INSIGHTS INTO SI ELECTROCHEMISTRY AND PORE GROWTH BY TRANSIENT MEASUREMENTS AND IMPEDANCE SPECTROSCOPY

G. Hasse, M. Christophersen, J. Carstensen, and H. Föll
Materials Science, Faculty of Engineering
Kaiserstr. 2, 24143 Kiel, Germany
Phone: + 49 431 77572-501
Email: gh@techfak.uni-kiel.de

Abstract

Silicon electrochemistry has many applications [1-4], but still a number of unanswered questions. This paper reports on experimental results of current transient measurements and impedance spectroscopy along the IV curve if the Si-HF system. The points of inflection of the IV-characteristics are found to be the interesting points, signaling the onset of new mechanisms supporting or suppressing current flow which are mostly coupled to oxide formation and/or dissolution. The results are interpreted as interactions of current bursts in time and in space. Following this interpretation, in-situ monitoring of pore nucleation and growth with FFT impedance spectroscopy, allowed to identify several phases of macropore formation and optimal growth conditions. In-situ monitoring of macropore growth may therefore be used to control nucleation and growth of macropores

Introduction

The quite complicated IV-characteristics of the Si-HF system with its two maxima (I_{PSL} and I_{OX}) and several points of inflections can be understood by assuming that the power transport ($U{\cdot}I$) across the Si electrolyte interface is maximized. Postulating a unique cycle for the local Si dissolution process (current burst), the IV curve can be interpreted as the potential dependent result of dominant interactions between current bursts, which support or suppress the electrochemical reactions. The onset of new types of interactions leads to a new trend in the IV curve characterized by a point of inflection. It then is not surprising that as an essential result of the transient current analysis the inflection points were found to be more fundamental for the understanding of the IV-curve than the extrema.

Experimental

For the experiments a custom-built potentiostat/galvanostat with a built-in FFT impedance spectrometer [5] was used. In aqueous electrolytes a Ag/AgCl-reference electrode was used whereas for the organic electrolytes a platinum electrode had to be employed. For the transient spectroscopy very diluted (0.05 w%) HF solution with NH_4Cl to enhance conductivity was used. A Stanford SR640 was applied for filtering the current transients and pre-amplifying the signal for impedance analysis. The electrolyte was circulated by a peristaltic pump at a constant (stabilized) temperature of 20^{o}C.

Transient spectroscopy

In growing an anodic oxide, a thin sub-stoichometric SiO_{2-x} layer exists at the Si-SiO_2 interface, called "sub-oxide", which contains charges. Dissolving the oxide purely chemically releases these charges as soon as the covering oxide has been dissolved. Switching the bias to open circuit potential, then produces a transient current peak $I(t)$ [6-13] which is a direct representation of the oxide thickness distribution $D(s)$ because the transient current I at time t is proportional to the surface area with an oxide thickness s which is dissolved exactly in the time interval t. The integral charge of this transient peak is proportional to the surface area which is covered with an oxide layer.

The oscillation regime

Macroscopic current and voltage oscillations [11,12] occur beyond the I_{ox}-Peak in the IV-characteristic. **Fig. 1a)** shows current oscillations which are damped due to the extremely low HF concentration of the electrolyte. The IV-curve of **Fig. 1b)** is constructed from these $I(t)$-curves plotting the current versus the potential after the oscillations have been damped away. In what follows we will only focus on three experimental results:

a) The first current oscillations in **Fig. 1a)** start at a potential of 1.7 V which is the point of inflection in **Fig. 1b)**.
b) The current noise decreases with increasing potential.
c) Simultaneously the (starting) amplitude ΔI of the oscillations increases *linearly* with the applied potential U.

Following the discussion above the statement a) implies that the onset of the oscillations supports the etch process. The results a)-c) can be well understood by interpreting macroscopic current oscillations as a synchronization process [10-13]. Specifying the underlying local oscillation processes as "current bursts" [11-13] which interact laterally and thus form (fluctuating) domains of phase coupled silicon dissolution (with a short period of growing oxide and a long period of dissolving oxide and always nearly the same oxide thickness within one domain), the current noise reflects the number of independent domains on the electrode surface. Increasing amplitude of the noise means increasing domain sizes (and thus fewer domains); at the onset of macroscopic oscillations only one domain is left. The strong (linear) dependence on the applied potential reflects the linear increase of the thickness of each oxide bump with applied potential, leading to a nearly linear increase of the lateral interaction of current bursts

and obviously (statement c)) to a linear increase with potential of the "coupling strength" of the one domain at the onset of macroscopic oscillations.
This synchronized growth and dissolution of the oxide layer thickness was directly measured by transient analysis before [12], showing in addition that the period of the oscillation as well as the frequency of the not synchronized domains (noise) depends linearly on the applied potential.

Electropolishing regime

Large domain sizes imply a complete oxide coverage at least for the area of a domain, and for thick oxides a complete oxide coverage of the electrode. As discussed above this coverage can be measured by the integral charge of a transient current peak. **Fig. 2** shows this transient charge for the intermediate regime between I_{PSL} and I_{OX} . The maximum of this curve can be interpreted as the potential at which complete oxide coverage occurs.
The reduction of the transient charge after the maximum with increasing potential does not imply a reduction of oxide coverage, but characterize a more sophisticated property of transient currents: current bursts through the oxide layer reduce the suboxide charge [12]. So the reduction of the transient charge after the maximum reflect the increasing number of current bursts through the closed oxide. Within the current burst model this is expected since a new oxide growth mode must start as soon as complete coverage of the electrode with oxide is achieved: Silicon oxide growth no longer nucleates on a free silicon surface, but through a closed oxide layer by an (field-strength induced) ionic break-through, i.e. a current burst.
The maximum of the transient charge of **Fig. 2** again coincides with the point of inflection of the *I-V* characteristics before the I_{OX} peak. This point of inflection, marking a trend to suppress current flow, is induced by the complete oxide coverage of the electrode.

PSL-Regime

Whereas the electrode is completely covered with oxide in the oscillation regime, in the low voltage part of the characteristic not much oxide is expected. And indeed, transient measurements showed only small peaks. In **Fig. 3** the ratio of the measured current of the $I(U)$ curve and the integral of the $I(t)$ transient curve (proportional to the suboxide charge and thus area coverage) is shown for the respective potential. Two intersecting straight lines are clearly visible. The point of intersection is exactly the point of inflection of the $I(U)$ curve before the

PSL peak. The current to charge ratio thus appears to be extremely sensitive to the process that causes a change in the curvature indicating current suppression. Within the current burst model these almost perfect straight lines as well as the change in the slope of both lines can be well understood when correlating the current $I(U)$ with the formation of oxide and the transient peak charge with the oxide coverage of the electrode. Two important results follow: i) Silicon oxide exists before the PSL peak; ii) the point of inflection before the PSL-peak is directly coupled to the onset of a lateral interaction of current bursts, i.e. the oxide bumps of the current bursts start to overlap at that point which hinders the current flow. The almost perfect linear relation with the applied potential U can be understood taking into account the linear increase of the oxide bump thickness with potential and the linear increase of domain sizes of current bursts with potential.

Monitoring of Macropores

As described in detail in [14,15], pore formation can be understood as a phase separation in space which is induced by the interaction of current bursts in time. The phase separation occurs because it allows for the same current, but at reduced potential in comparison to the nucleation phase, i.e. before pores are nucleated. In consequence, pore formation leads to a reduction of the effective resistance of the system.

The formation and growth of pores dependents on many parameters [1-4], and one is the current usually kept constant be controlling the voltage or, in the case of n-type Si, the intensity of the illumination. When growing pores, it would be advantageous if all parameters could be held at optimal values, which might need continuos adjustments of current, voltage, illumination etc.. To do this in an effective way, pore growth must be monitored in-situ by measuring quantities that give direct information about the conditions at the pore tip. We have applied FFT impedance spectroscopy to address this task. Though we could not measure in-situ the complete spectrum containing all frequencies needed for the usual semicircles in a Nyquist plot (it takes too long), the desired information could still be obtained since it proved to be sufficient to log the movement of one single point in the spectrum (i.e. at one optimal frequency) with the etching time. This represent possible shifts in the complete Nyquist provided the shape is not altered significantly during the etching. This, as ascertained in several complete measurements, was generally not the case.

Two representative measurements of extreme cases are presented in **Fig. 4**. The first measurement shows the real part of the impedance spectrum at the frequency of 2.6 kHz during a

typical macropore growth experiment in p-type Si yielding "good", i.e. stable and uniform pores. (**Fig. 4a-i)**). In the corresponding SEM picture it can be seen that pores have been etched indeed, showing “bottlenecks“ in their upper parts. This is a common feature in well etched macropores. Three different regions can be identifies in **Fig. 4a-ii)**. First a strong decrease, then a slight curvature, followed by an increase that in the first part is nearly linear. The cell potential shows pronounced changes, too during the etching under galvanostatic conditions (**Fig. 4a-iii)**) but in a shape quite different from the Z_{Re}-Plot.

Fig. 4b) shows the results for “bad” pores. The $Z_{re(t)}$-Plot as well as the $U(t)$-plot are quite different from the first case. The SEM picture shows irregular ("bad") pores without bottlenecks and a very rough surface. The real part of the impedance now is decreaing in a linear way, whereas the voltage drops significantly before increasing again slightly.

The pronounced differences in the time development of the impedance may be tentatively explained as follows: In **Fig. 4a)** the initial drop in resistance may be attributed to the breaking of the H-coverage, i.e. in removing the passivation layer. This also shows up in the respective $U(t)$-curve. The first dotted line in **Fig. a-ii)** signifies the end of H-bond breaking. What follows is the nucleation phase with minimal transfer resistance, signaling that the pores arrange in an advantageous way and the electrochemical reaction is optimized.

The increase of the resistance after the second dashed line then is due to the growing distance l between the counter electrode and the pore tip, increasing the over-all resistance $R=\rho l/A$. In the voltage, on the other hand, changes in capacity are visible as well, inseparable from the voltage drops due to resistance change, and that is why the real part of the impedance spectrum yields more useful information.

For "bad" pores the drop in resistance can now be interpreted as a result of the increasing surface area. Though the $U(t)$-plot looks different, there still are some similarities with the one depicted in **Fig. 4a**. The strong initial drop is due to the H-bond breaking as before. But the transition to the rising part is far less pronounced and the rise itself is weaker. Both is explained by incomplete and ongoing nucleation. As the nucleation phase is never really finished, the surface roughens, again increasing the area and decreasing the resistance.

The key to controlling pore growth now seems to be the control of the transfer resistance of the electrochemical reaction. It should be minimized as shown in the regime between the dotted lines in Fig. 4a-ii) and this can be done by adjusting controllable parameters as the current, or the voltage. This might be implemented in a closed control loop, but what can be achieved with this technique still remains to be seen.

Conclusions:

The current burst model is capable of explaining salient features of the *I-V*-characteristics. The measurements shown here support this model and provide powerful input for the development of a quantitative theory. In particular, the measurements support the interpretation that the oxide grown by current bursts governs the shape of the characteristic and that the points of inflection are the more interesting points in the *I-V*-characteristics. In-situ impedance measurements interpreted in terms of the current burst model provide additional data for the development of the model, moreover, the might evolve to a powerful tool for controlling the growth of pores

References:

[1] L.T. Canham, *Appl. Phys. Lett*., **57**,(1990) 1046

[2] V. Lehmann, U. Gösele, *Appl. Phys. Lett*., **58**,(1991) 856

[3] H. Föll, *Appl. Phys*. **A 53**,(1991) 8

[4] R.L. Smith, S.D. Collins, *J. Appl. Phys*. **71** (8) (1992)

[5] G.S. Popkirov, R.N. Schindler: *Rev. Sci. Instrum*., **63**, 1992

[6] C. Serre, S. Barret, R. Herino, *J. Electrochem. Soc*. **141** (8), (1994) 2049

[7] M. Matsumura, S. R. Morrison, *J. Electroanal. Chem*. **147**, (1983) 157

[8] H. Gerischer, M. Lübke, *Ber. Bunsenges. Phys. Chem*. **92**, (1988) 573

[9] J. Rappich, H.J. Lewerenz, *J. Electrochem. Soc*., **142** (4), (1995) 1233

[10] F. Ozanam, J. N. Chazalviel, A. Radi, M. Etman, *Ber. Bunsenges. Phys. Chem*., **95** (1), (1991) 98

[11] J. Carstensen, R. Prange, H. Föll, *J. Electrochem. Soc*., **146** (3),(1999) 1134

[12] J. Carstensen, R. Prange, G.S. Popkirov, H. Föll, *Appl. Phys*. **A 67**, (1998) 459

[13] G. Hasse, J. Carstensen, G. Popkirov, H. Föll, *Mat. Sci. and Eng*., **B69-70**, (2000) 188

[14] H. Föll, J. Carstensen, M. Christophersen, G. Hasse, *this proceedings*

[15] J. Carstensen, M. Christophersen, G. Hasse, H. Föll, *this proceedings*

[16] V.P. Parkhutik, *J. Porous Mat*., **7**, (2000) 97

Captions

Fig.1: a) The $I(t)$-curves for different voltages on the decaying region of the I_{Ox}-peak. Beyond this peak lies the well known oscillations regime and the first signs of damped oscillations can be observed at approximately 1.7 V.
b) Decaying part of the I_{Ox}-peak obtained by plotting the equilibrium currents from **Fig. 1a**.

Fig. 2: The transient charge (integral of the *I(t)*-transient) plotted versus the potential has a maximum at 1 V. This is due to complete oxide coverage. The following fall must be accounted to breakthrough losses.

Fig. 3: Ratio of the external current and the total charge measured by integrating the current transient obtained at the corresponding potential (p-Si, aqueous electrolyte with low (0.05 w%) HF concentration).

Fig. 4: a) Pore etching under galvanostatic conditions, p-Si 7-12Ωcm, 4mA/cm^2, electrolyte DMSO, 4w%HF, Tetrabutylammonium perchlorate to reduce resistance.
i) SEM Photograph (cross section) of pores in p-Si. Typical bottlenecks are visible near the surface.
ii) Real part of the FFT impedance at 2.6 kHz.
iii) Cell potential during pore etching.
b) Pore etching under galvanostatic conditions, p-Si 10-20Ωcm 1.35mA/cm^2, electrolyte DMF, 4w%HF
i) SEM Photograph (cross section) of low quality pores. The surface is very rough.
ii) Real part of the FFT impedance at 2.6 kHz.

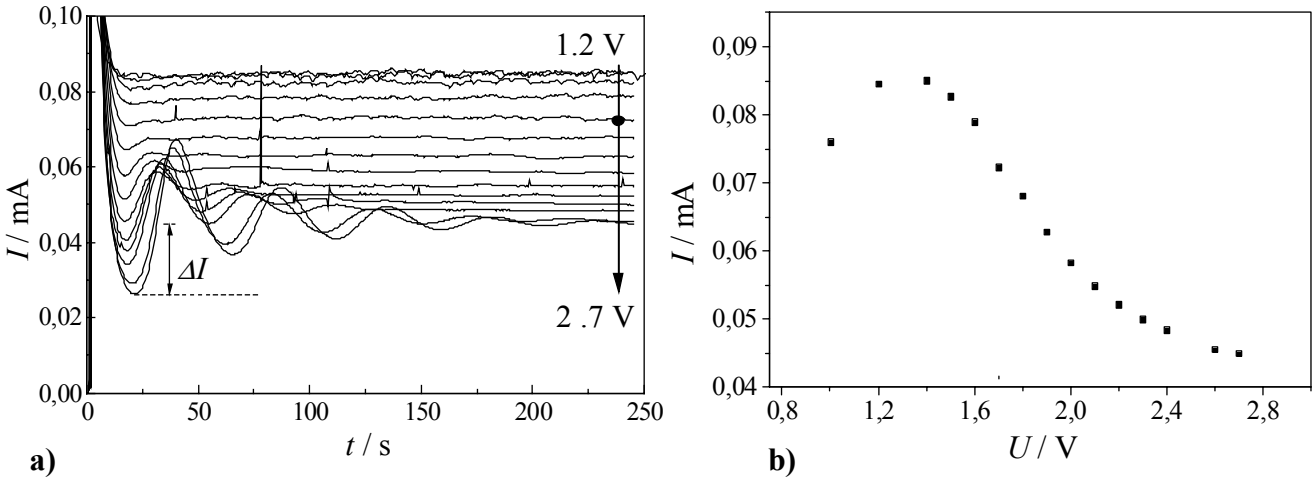
0,10
0,08
0,06
0,04
0,02
0,00
I / mA
1.2 V
ΔI
2 .7 V
0
50
100
150
200
250
t / s
a)
0,09
0,08
0,07
0,06
0,05
0,04
I / mA
0,8
1,2
1,6
2,0
2,4
2,8
U / V
b)

Fig. 1

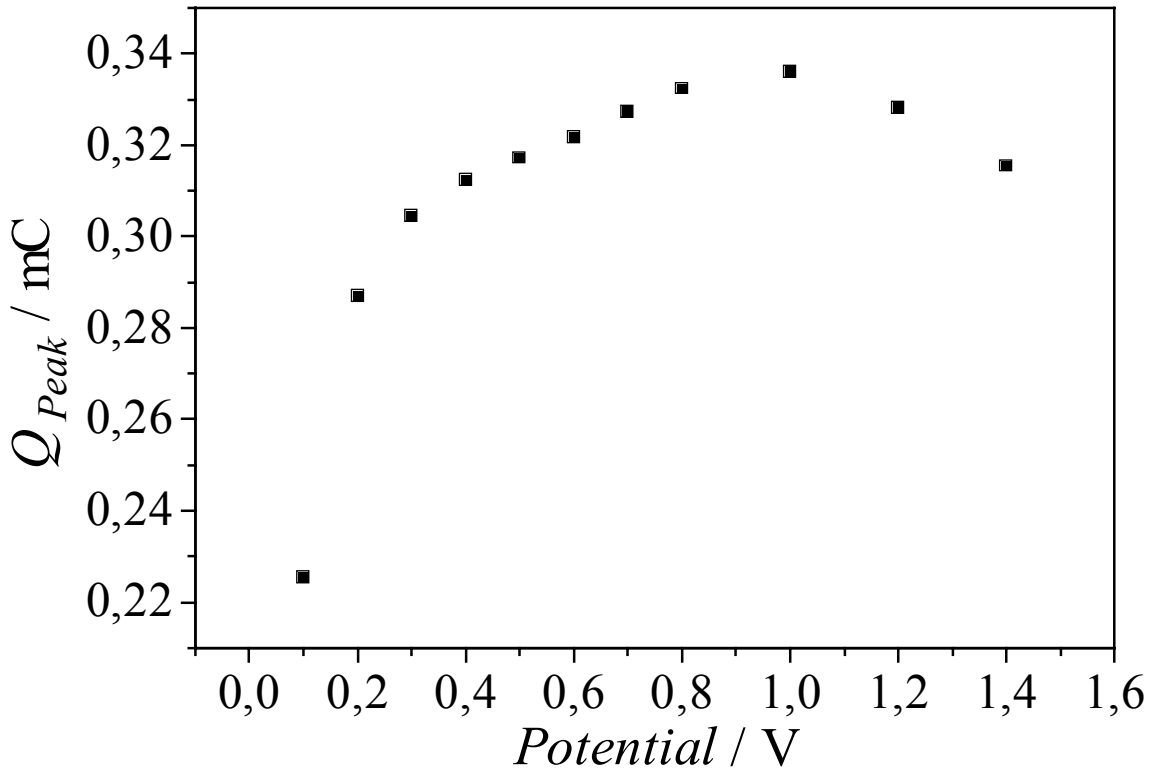
0,34
0,32
0,30
0,28
0,26
0,24
0,22
Q Peak / mC
0,0
0,2
0,4
0,6
0,8
1,0
1,2
1,4
1,6
Potential / V

Fig.2

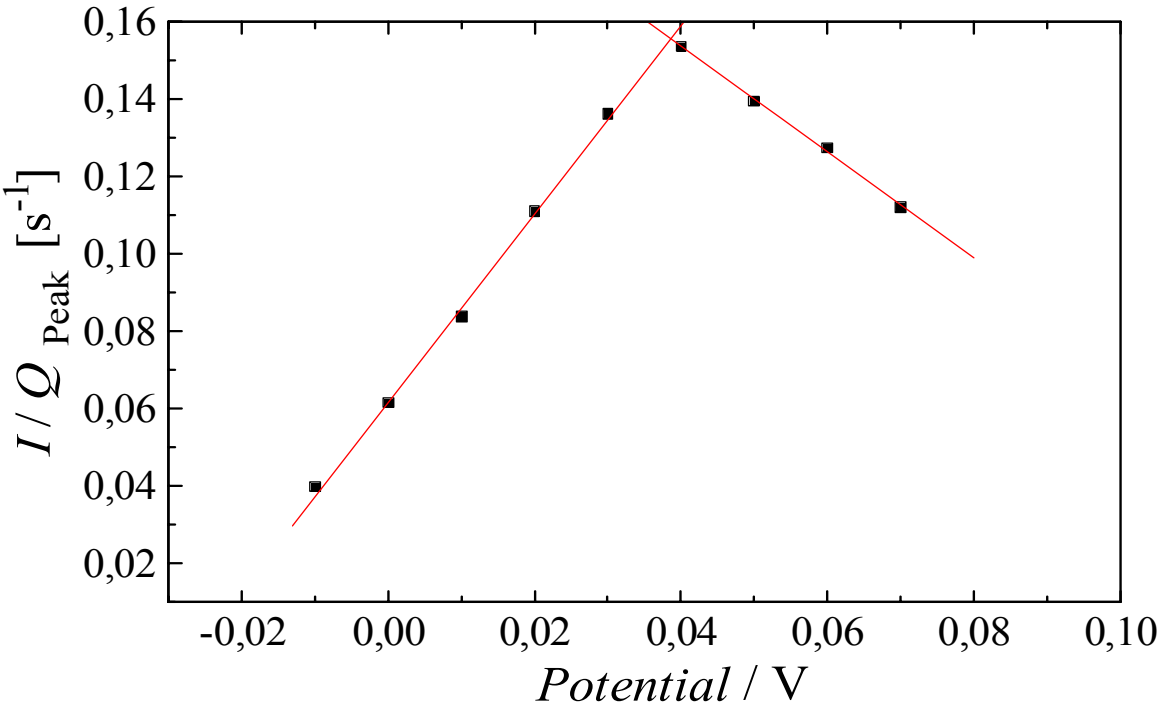
0,16
0,14
0,12
0,10
0,08
0,06
0,04
0,02
I / Q Peak [s-1]
-0,02
0,00
0,02
0,04
0,06
0,08
0,10
Potential / V

Fig.3

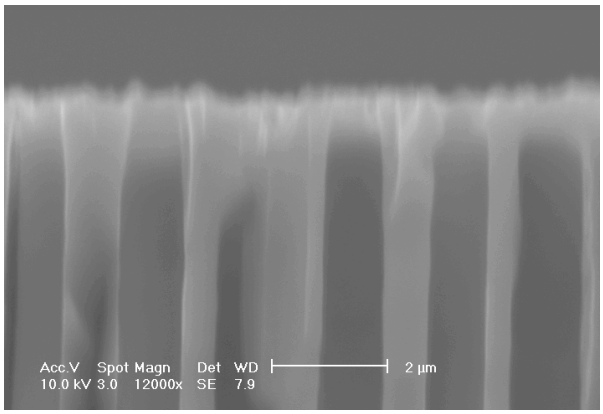

i)

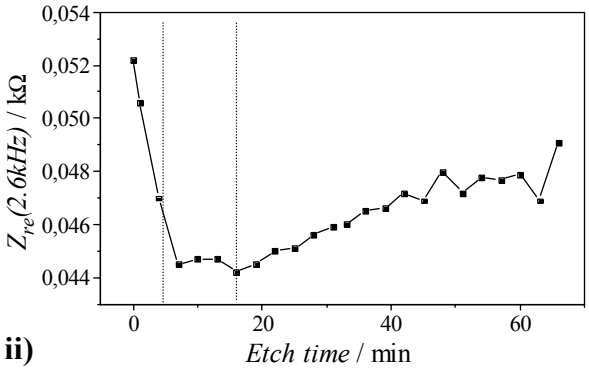

ii)

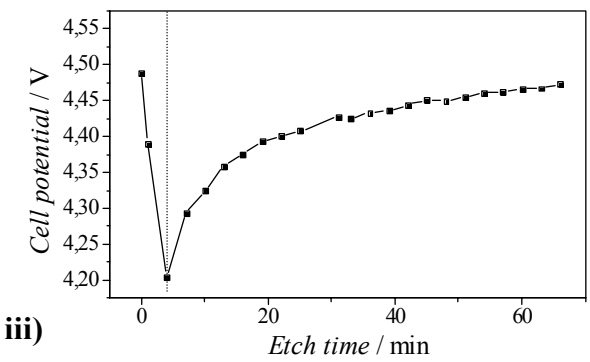

iii)

a)

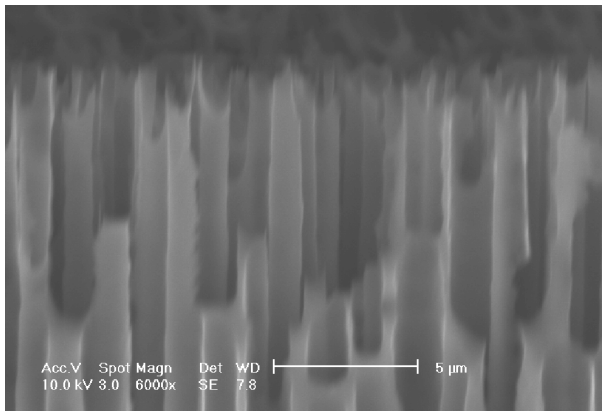

i)

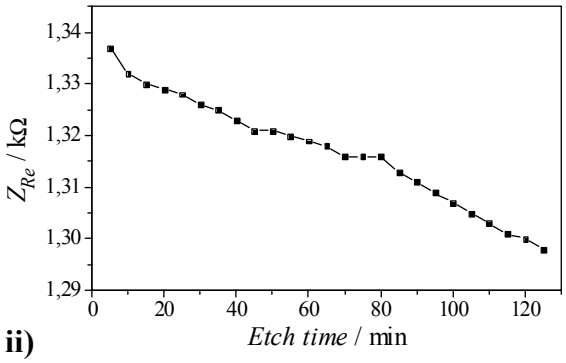

ii)

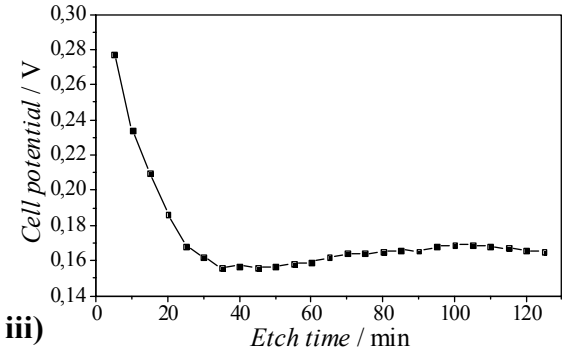

iii)

b)

Fig.4